UNIVERSITY OF BATH

Citation for published version:
Crespo-otero, R & Walsh, A 2015, 'Variation in Surface Ionization Potentials of Pristine and Hydrated BiVO4', Journal of Physical Chemistry Letters, vol. 6, no. 12, pp. 2379-2383. https://doi.org/10.1021/acs.jpclett.5b00966

DOI:
10.1021/acs.jpclett.5b00966

Publication date:
2015

Document Version
Publisher's PDF, also known as Version of record

Link to publication

Publisher Rights
CC BY

University of Bath

Variation in Surface Ionization Potentials of Pristine and Hydrated BiVO$_4$

Rachel Crespo-Otero*,[†] and Aron Walsh[‡]

[†]School of Biological and Chemical Sciences, Queen Mary University, London E1 4NS, United Kingdom
[‡]Department of Chemistry, University of Bath, Claverton Down, Bath BA2 7AY, United Kingdom

S *Supporting Information*

ABSTRACT: Bismuth vanadate (BiVO$_4$) is a promising material for photoelectrochemical water splitting and photocatalytic degradation of organic moieties. We evaluate the ionization potentials of the (010) surface termination of BiVO$_4$ using first-principles simulations. The electron removal energy of the pristine termination (7.2 eV) validates recent experimental reports. The effect of water absorption on the ionization potentials is considered using static models as well as structures obtained from molecular dynamics simulations. Owing to the large molecular dipole of H$_2$O, adsorption stabilizes the valence band edge (downward band bending), thereby increasing the ionization potentials. These results provide new understanding to the role of polar layers on complex oxide semiconductors, with importance for the design of efficient photoelectrodes for water splitting.

Enormous efforts and resources have been put into the study of photoelectrochemical water splitting on semiconductor surfaces since the seminal work on TiO$_2$ electrodes in the 1970s.[1−3] No single material has been found to achieve water oxidation *and* reduction under visible light at a rate that is commercially viable. A common architecture for the water splitting process, called Z-scheme or photosynthetic cell,[4,5] is a tandem system composed by an n-type photoanode and a p-type photocathode, allowing a better efficiency for the whole process. Oxidation of water requires the participation of four electrons and is consequently limited by the kinetics of the carriers, which can be sensitive to the surface structure and surface potential of the photoanode.

Bismuth vanadate (BiVO$_4$) is one of the most promising metal oxides to be used as a photoanode in the Z-scheme and as a photocatalyst for degradation of organic compounds.[6−8] BiVO$_4$ exists in three polymorphs: orthorhombic pucherite, monoclinic clinobisvanite and tetragonal dreyerite. While the optical band gap of the orthorhombic phase is larger (around 2.9 eV), the tetragonal and monoclinic phases have similar band gaps (between 2.3 and 2.5 eV). The monoclinic phase is the thermodynamically most stable and exhibits the best photocatalytic properties, as well as a higher hole mobility in comparison to the tetragonal phase.[9]

Scheme 1 shows the alignment of energy levels for the monoclinic BiVO$_4$ phase based on recent data from photoemission spectroscopy.[10] The valence band maximum (**VBM**) is in a favorable position for water oxidation. A small overpotential (electrochemical bias) is required to reduce water since the conduction band minimum (**CBM**) is below the H$^+$/H$_2$ potential. A recent study showed that quantum-sized BiVO$_4$ can decompose water in H$_2$O and O$_2$ without the use of a cocatalyst, which can be understood considering the

Scheme 1. Alignment of Energy Levels of Monoclinic BiVO$_4$ with Respect to the Vacuum Level[a]
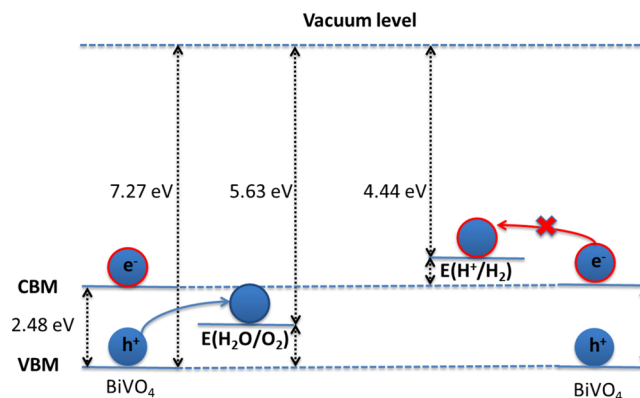
[a]The values were taken from ref 10 based on photoemission experiments.

destabilization of the **CBM** energy (decrease in electron affinity) level due to quantum confinement effects.[11]

In spite of its attractive features, in the absence of an extra catalyst, crystalline BiVO$_4$ shows a modest photoelectrochemical performance, with small current densities and low overall conversion efficiencies.[7,12] Poor transport properties, significant electron−hole recombination and slow O$_2$ evolution are the main limiting factors associated with its poor catalytic behavior. Weak hole localization (large hole-polaron) and a small electron polaron have been suggested, which could explain

Table 1. Calculated Energy Gaps, Ionization Potentials (IP), and Electron Affinities (EA) in eV for the (110) Surface of BiVO$_4$ Formed of n Bilayers^a

slab models	E_{gap}		IP^{BiVO_4}		EA^{BiVO_4}	
n	PBE	PBEsol	PBE	PBEsol	PBE	PBEsol
1	2.08 (3.48)^b	2.06	7.18 (8.10)^b	7.23	5.18 (4.62)^b	5.10
2	2.04	2.02	7.19	7.24	5.22	5.15
3	2.04	2.02	7.18	7.24	5.22	5.15
4	2.04	2.02	7.19	7.24	5.22	5.15

^{a}Values are compared for two exchange-correlation treatments (PBE and PBEsol) within density functional theory. ^{b}Values obtained with the HSE06 hybrid functional (fully optimized structure).

the slow electron mobility and the significant electron−hole recombination.[9,13,14] Different strategies like facet engineering; morphology control, doping, and the use cocatalyst have been explored to obtain better efficiencies.[15−17]

The combination of experiment and density functional theory (DFT) calculations have shown that the (010) surface of BiVO$_4$ is the most stable with a significant area exposed to the solvent.[18−20] Water absorption on semiconductor surfaces affects the electronic structure and consequently the photo-catalytic and electrocatalytic properties. In this Letter, we quantify the effects of the water at the contact with the (010) surface of BiVO$_4$ on the ionization potentials using electronic structure and molecular dynamic simulations. Our results provide an understanding of the role of solvent on the electronic structure of semiconductor surfaces, which have implications for the design of optimal photoanodes. At the same time, absorbed water layers can serve as models for polar layers deposited on the oxide surfaces.

The quantitative prediction of absolute electronic energy levels is challenging for solid-state electronic structure modeling.[21] The most common approach consists of the alignment of the electronic bands with respect to the vacuum level using slab (pseudo-2D periodic) models.[21] To analyze the alignment of the energy levels and compare with the most recent experimental data, we consider the (010) surface using slab models that contain stoichiometric (BiVO$_4$)$_{4n}$ units with n = 1,2,3,4. We focused on the most stable termination, consisting of charge-neutral quadrupolar layers, which expose the oxygen atoms. The surface energies are 0.30 and 0.20 J/m^2 values with PBEsol and PBE exchange-correlation functionals, respectively (Supporting Information Table S1). The small surface energies confirm the high stability of the (010) surface in agreement with previous studies.[20]

Recent photoemission experiments placed the upper valence band 7.27 eV below the vacuum and the lower conduction band at 4.79 eV (Scheme 1).[10] The quasi-particle band gap obtained from X-ray emission (XES) and absorption (XAS) is 2.48 eV;[10] previous X-ray experiments reported a value of 2.38 eV.[22] It is well-known that gradient-corrected DFT functionals underestimate the bands gaps of insulators. The converged gap for the surface model is 2.04 eV (2.02 eV) with PBE (PBEsol), which is similar to the values obtained for the bulk material (Table 1). In contrast, for the same geometry, the band gaps obtained with the hybrid functionals HSE06 and PBE0 (25% exact exchange) are 3.15 and 3.10 eV, respectively. Kweon et al. found only 5% of exact exchange is required to obtain a band gap of 2.5 eV for BiVO$_4$.[14] This unusual feature may be related to the chemical makeup of the band edge states: a smaller derivative discontinuity is found for metal oxides formed of post-transition metals with valence ns^2 orbitals (here Bi 6s^2).

The comparison between the experimental data and the calculated band edge positions (Table 1) indicates that the underestimation of the electronic band gap is related to the under-stabilization of the **CBM**. The good agreement of the ionization potentials with these functionals shows that the **VBM** orbitals are well described with these GGA functionals. By alignment of the core levels with the periodic solid, the predicted bulk ionization potentials are 7.24 and 7.30 eV with PBE and PBEsol functionals, respectively (Table S2). The corresponding electron affinities are 5.21 and 5.27 eV, only slightly shifted from the values obtained for the surface models (5.10 and 5.18 eV) as a consequence of the small band bending energies.

The evaluation of the energy level alignments is more involved for interfaces and electrode models.[23] Considering the good agreement between the ionization potentials computed with the PBE functional and the experimental values, we used this functional to evaluate the effect of the water at the contact with the (010) surface on the ionization potentials. We considered four models. **I** − *bismuth*: one water molecule interacting with the Bi surface atoms. **II** − *oxygen*: one water molecule interacting with the O surface atoms at typical hydrogen bond distances. **III** − *monolayer*: molecular dynamics simulations of BiVO$_4$ in contact with liquid water, where two molecules are stabilized by a hydrogen bond resembling the dimer of water (cell and supercell models were considered, with similar geometries and energetics, Figure 1). **IV** − *frozen liquid*: the semiconductor surface in contact with 14 molecules of water (to approximate the density of liquid water for a slab model an interlayer spacing of 15 Å), and a vacuum of 15 Å (see Figure 1).

In order to analyze the structure of water interacting with the semiconductor surface, molecular dynamics of model **III** were
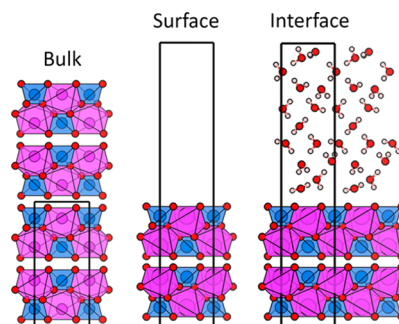

Figure 1. Models for the interaction between a layer of water and the BiVO$_4$ (010) surface: (a) the bulk crystal structure; (b) the (010) surface terminated with vacuum; (c) the (010) surface in contact with water. The Bi−O polyhedra are shaded pink, with the V−O polyhedral shaded blue.

Table 2. Calculated Properties for the BiVO$_4$ Surfaces: Monolayer and Frozen-Liquid Models^a

	E_{gap}	IP^{BiVO_4}	ΔIP^{BiVO_4}	IP^{BiVO_4/H_2O}	$W_e^{BiVO_4/H_2O} - W_e^{BiVO_4}$	$e_0 U_{VBM}$
monolayer	2.18	7.35	0.17	6.53	0.81	2.90
frozen-liquid	2.16	7.32	0.14	6.22	1.11	2.88

^{a}All quantities are in eV. IP^{BiVO_4} is the ionization potential associated with the surface in contact with vacuum, and the IP^{BiVO_4/H_2O} corresponds to the ionization potential of the surface in contact with water. ΔIP^{BiVO_4} is the difference between the IP^{BiVO_4} of the slab model and the ionization potential of the bare surface (Table 1). $W_e^{BiVO_4/H_2O} - W_e^{BiVO_4}$ is the work to transport an electron from the semiconductor to the solution. $e_0 U_{VBM}$ is the electrochemical potential with reference to the hydrogen electrode (Supporting Information).
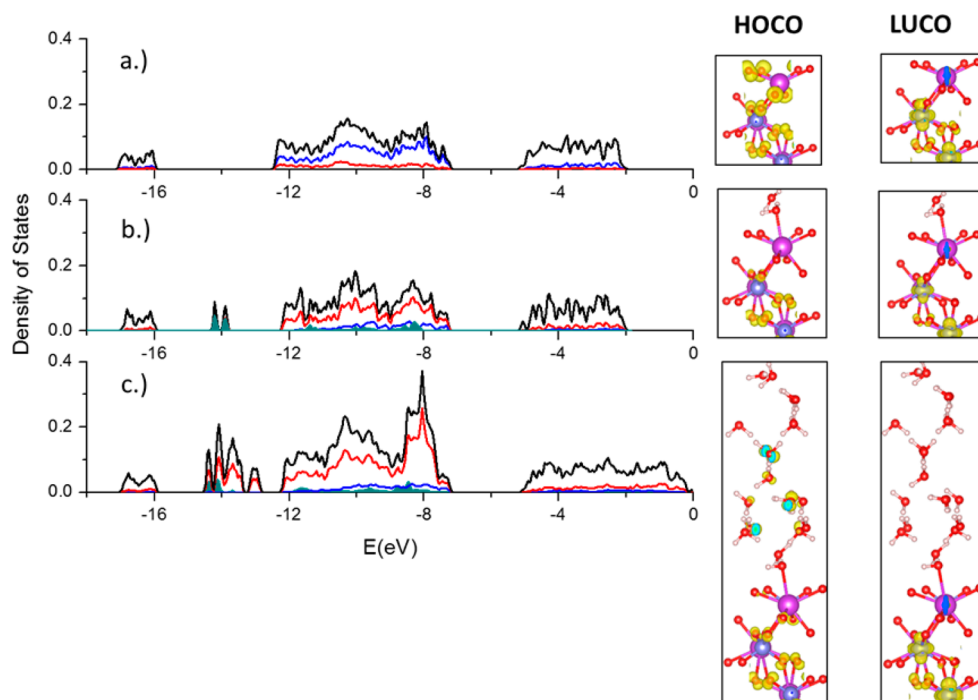

Figure 2. Electronic density of states scaled with respect to the semicore Bi 5d band (not shown) for (a) a pristine slab model, (b) monolayer (model **III**), and (c) frozen-liquid (model **IV**). The highest occupied state is set to $-IP^{BiVO_4}$ (eV). The electron density from the highest occupied (HOCO) and lowest unoccupied (LUCO) crystal orbitals are represented in the right panel.

performed at 298 K. Ten snapshots from the dynamics of the monolayer model were considered in order to evaluate the effect of water mobility and surface relaxation on the ionization potentials (more details can be found in the Supporting Information). More comprehensive molecular dynamics simulations and dynamic local structure analysis will be performed in future work.

The absorption of one water molecule on the Bi and V sites stabilizes the system by −0.48 and −0.22 eV, respectively (models **I** and **II**). The absorption energy of the dimer (model **III**) is −0.98 eV; the process is thermodynamically favorable. For the monolayer model, a distorted hexagonal structure of hydrogen bonds on the surface is found, where water absorbs on the Bi sites. The second water molecule is located at hydrogen bond distances of 1.74 and 1.85 Å from the O−V (Figure 1). The frozen-liquid model shows a similar pattern for the water absorbed on the surface, but with Bi···OH$_2$ and VO··· H−OH distances larger about 0.1 Å. On the other hand, the water−water distance is shorter because of the effect of the surrounding water molecules.

The first step of the water oxidation process is the H dissociation. Consequently, the presence of a second molecule interacting with the adsorbed water could be relevant for the mechanism of water oxidation on BiVO$_4$ surfaces. Our molecular dynamics simulations for the monolayer and liquid

water did not show any dissociative event. Earlier DFT calculations also reported the nondissociative nature of the water absorption on pristine BiVO$_4$ surfaces.[19,24,25]

Table 2 shows the effect of water on the ionization potentials for models **III** and **IV**. The interaction between water and the semiconductor slightly increases the IP^{BiVO_4} ionization potential with respect to the bare surface (Table 1) from 7.18 eV to 7.35 and 7.32 eV for the monolayer and frozen-liquid models, respectively. This is a consequence of the stabilization of the upper valence band because of the interaction with the solvent. At the same time, the band gap increases by about 0.1 eV for both models. While the ionization potentials of the surface in contact with vacuum are similar, the ionization potential associated with the surface hydrated surface (IP^{BiVO_4/H_2O}) changes from 6.53 to 6.22 eV from the monolayer to the frozen-liquid. Consequently, it is more difficult to bring an electron to the hydrated surface when the concentration of molecules of water is increased.

Understanding the effect of water on the ionization potentials is useful to analyze the electronic density of states and the chemical nature of the band edge orbitals (Figure 2). As for the bulk material and the pristine (010) surface,[26] the valence band is dominated by the 2p oxygen orbitals, and the conduction band has a significant contribution from the V 3d orbitals. In the case of hydrated surface models, a group of

additional states corresponding to the combination of O 2s of water appears around −7 eV. This band is displaced about 2 eV from the band composed by the O 2s of the semiconductor due to the difference in chemical environment. The O 2s band is broader for the frozen-liquid because of the distribution of local H_2O environments and some contributions from the H 1s orbitals from the hydrogen bond network. The orbitals from absorbed water molecules are more stable than the others coming from the nonabsorbed water molecules. Another interesting feature of the frozen-liquid is the broader conduction band; while the orbitals close to the lower conduction band are basically V 3d, the higher energy orbitals are a combination of Bi 6p and O 2p.

Upon water absorption, a fraction of the highest-occupied electron density is transferred from the surface to the subsurface semiconductor layers (see Figure 2). This process stabilizes the upper valence band and explains why the ionization potentials for the monolayer and frozen-liquid models increase with respect to the bare surface model. There is a small influence of water on the lower conduction band because these orbitals have a small contribution from the surface. The addition of a polar layer on the surface of $BiVO_4$ could potentially shift the energy levels without an important contribution of the orbitals of the layer to the band edge orbitals. The use of polar layers like FeOOH, NiO and NiOOH, which accelerate the O_2 release kinetics, could behave similarly.[7,27]

The dynamics of the water at the contact with the surface includes the desorption−absorption processes. The mobility of water molecules could displace the states from the absorbed water to the edge of the band and could also help also to stabilize the trap states. Recent experiments show the role of the hole and electron trap states in the photophysics of $BiVO_4$.[28] To provide insight into the effect of the dynamics of water into the ionization potentials, 10 snapshots from the molecular dynamics were analyzed. During the dynamics, all atoms were allowed to relax, and then the effect of the surface relaxation was taken into account as well as the dynamics of the water molecules. The energy levels were aligned with respect to the calculated vacuum level in each case (Figure 3).

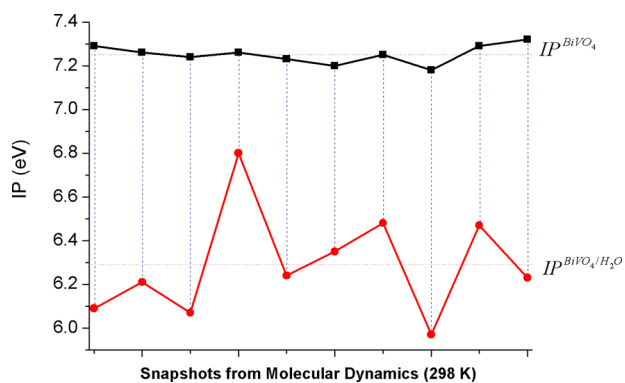The band gaps of the considered snapshots are in general smaller than those obtained from the static models, which can be associated with the destabilization of upper valence orbitals (decrease in ionization potential) due to the deviation from the equilibrium geometry (Table 2). The calculated ionization potentials are still larger than those obtained for the bare surfaces (Table 1). IP^{BiVO_4/H_2O} depends strongly on the structure of water; consequently, their values show larger oscillations than the obtained for other properties. The effect of orientational disorder on the evaluation of ionization potentials is discussed in refs 29 and 30. In all cases, the IP^{BiVO_4/H_2O} values are smaller than the obtained for the static monolayer model and closer to the values obtained for the frozen-liquid. Some orientational disorder of the water dipoles is required to reproduce the instantaneous changes in the electrostatic potential during the liquid dynamics. The work to bring an electron from the bare to the hydrated surfaces ($W_e^{BiVO_4/H_2O} - W_e^{BiVO_4}$) also oscillates significantly from 0.5 to 1.2 eV, which is also correlated to the variations of the water structure during the dynamics.

The IP^{BiVO_4} values are in good agreement with the data reported by Kim and Choi[7] for unmodified $BiVO_4$ (7.2−7.5 eV at pH = 7). They observed an increase of the flat band potential using layers of FeOOH and NiOOH. Our calculations suggest that the deposition of polar layers on $BiVO_4$ has an impact on the electronic structure of the semiconductor. The increasing of the ionization potential can be associated with a more efficient electron−hole separation, which is one of the effects of polar oxide layers.[7,27,31] Consequently, more efficient $BiVO_4$-based materials could be designed tuning the surface ionization potentials using polar layers. Given the layered structure of this material, a polar substitution (e.g., F incorporation) in a subsurface layer could be used to provide a chemically robust modification, which we aim to explore in future studies.

In conclusion, first-principles electronic structure calculations validate the measured ionization potential of bismuth vanadate, and provide new insights into the role of water on the surface electronic structure. The main effect of the interaction between water and the $BiVO_4$ surface is the stabilization of the upper valence band. As a consequence, the ionization potentials increase with respect to the bare surfaces. This effect was found for all considered models, as well as when molecular dynamics allowed the motion of surface atoms and water molecules. These results can contribute to a better understanding of the behavior of photoanodes that are mostly in contact with water and the effect of polar layers deposited on semiconductor surfaces.

■ ASSOCIATED CONTENT

ⓢ Supporting Information

Additional material is provided in the Supporting Information, including computational details and description of models. The Supporting Information is available free of charge on the ACS Publications website at DOI: 10.1021/acs.jpclett.5b00966.

■ AUTHOR INFORMATION

Corresponding Author

*E-mail: r.crespo-otero@qmul.ac.uk.

Notes

The authors declare no competing financial interest.

Figure 3. Ionization potentials (IP) with respect to the vacuum level calculated for 10 snapshots (ordered by time) obtained from the 298 K dynamics of a water monolayer on the surface of $BiVO_4$ (PBE functional). All values are in eV. The vertical lines represent the work to transport an electron from the bare material to the hydrated surface ($W_e^{BiVO_4/H_2O} - W_e^{BiVO_4}$).

■ REFERENCES

(1) Fujishima, A.; Honda, K. Electrochemical Photolysis of Water at a Semiconductor Electrode. *Nature* **1972**, *238*, 37−38.

(2) Peter, L. M.; Upul Wijayantha, K. G. Photoelectrochemical Water Splitting at Semiconductor Electrodes: Fundamental Problems and New Perspectives. *ChemPhysChem* **2014**, *15*, 1983−1995.

(3) Protti, S.; Albini, A.; Serpone, N. Photocatalytic Generation of Solar Fuels from the Reduction of H_2O and CO_2: A Look at the Patent Literature. *Phys. Chem. Chem. Phys.* **2014**, *16*, 19790−19827.

(4) Grätzel, M. Photoelectrochemical Cells. *Nature* **2001**, *414*, 338−344.

(5) Maeda, K. Z-Scheme Water Splitting Using Two Different Semiconductor Photocatalysts. *ACS Catal.* **2013**, *3*, 1486−1503.

(6) Hisatomi, T.; Kubota, J.; Domen, K. Recent Advances in Semiconductors for Photocatalytic and Photoelectrochemical Water Splitting. *Chem. Soc. Rev.* **2014**, *43*, 7520−7535.

(7) Kim, T. W.; Choi, K.-S. Nanoporous $BiVO_4$ Photoanodes with Dual-Layer Oxygen Evolution Catalysts for Solar Water Splitting. *Science* **2014**, *343*, 990−994.

(8) Murcia-López, S.; Villa, K.; Andreu, T.; Morante, J. R. Partial Oxidation of Methane to Methanol Using Bismuth-Based Photo-catalysts. *ACS Catal.* **2014**, *4*, 3013−3019.

(9) Kweon, K. E.; Hwang, G. S. Structural Phase-Dependent Hole Localization and Transport in Bismuth Vanadate. *Phys. Rev. B* **2013**, *87*, 205202.

(10) Cooper, J. K.; Gul, S.; Toma, F. M.; Chen, L.; Glans, P.-A.; Guo, J.; Ager, J. W.; Yano, J.; Sharp, I. D. Electronic Structure of Monoclinic $BiVO_4$. *Chem. Mater.* **2014**, *26*, 5365−5373.

(11) Sun, S.; Wang, W.; Li, D.; Zhang, L.; Jiang, D. Solar Light Driven Pure Water Splitting on Quantum Sized $BiVO_4$ without Any Cocatalyst. *ACS Catal.* **2014**, *4*, 3498−3503.

(12) Ma, Y.; Pendlebury, S. R.; Reynal, A.; Le Formal, F.; Durrant, J. R. Dynamics of Photogenerated Holes in Undoped $BiVO_4$ Photo-anodes for Solar Water Oxidation. *Chem. Sci.* **2014**, *5*, 2964−2973.

(13) Kweon, K. E.; Hwang, G. S. Surface Structure and Hole Localization in Bismuth Vanadate: A First Principles Study. *Appl. Phys. Lett.* **2013**, *103*, 131603.

(14) Kweon, K. E.; Hwang, G. S.; Kim, J.; Kim, S.; Kim, S. Electron Small Polarons and Their Transport in Bismuth Vanadate: A First Principles Study. *Phys. Chem. Chem. Phys.* **2014**, *17*, 256−260.

(15) Park, Y.; McDonald, K. J.; Choi, K.-S. Progress in Bismuth Vanadate Photoanodes for Use in Solar Water Oxidation. *Chem. Soc. Rev.* **2013**, *42*, 2321−2337.

(16) Huang, Z.-F.; Pan, L.; Zou, J.-J.; Zhang, X.; Wang, L. Nanostructured Bismuth Vanadate-Based Materials for Solar-Energy-Driven Water Oxidation: A Review on Recent Progress. *Nanoscale* **2014**, *6*, 14044−14063.

(17) Sun, S.; Wang, W. Advanced Chemical Compositions and Nanoarchitectures of Bismuth Based Complex Oxides for Solar Photocatalytic Application. *RSC Adv.* **2014**, *4*, 47136−47152.

(18) Li, R.; Zhang, F.; Wang, D.; Yang, J.; Li, M.; Zhu, J.; Zhou, X.; Han, H.; Li, C. Spatial Separation of Photogenerated Electrons and Holes among {010} and {110} Crystal Facets of $BiVO_4$. *Nat. Commun.* **2013**, *4*, 1432.

(19) Yang, J.; Wang, D.; Zhou, X.; Li, C. A Theoretical Study on the Mechanism of Photocatalytic Oxygen Evolution on $BiVO_4$ in Aqueous Solution. *Chemistry* **2013**, *19*, 1320−1326.

(20) Zhao, Z.; Li, Z.; Zou, Z. Structure and Energetics of Low-Index Stoichiometric Monoclinic Clinobisvanite $BiVO_4$ Surfaces. *RSC Adv.* **2011**, *1*, 874−883.

(21) Walsh, A.; Butler, K. T. Prediction of Electron Energies in Metal Oxides. *Acc. Chem. Res.* **2014**, *47*, 364−372.

(22) Payne, D. J.; Robinson, M. D. M.; Egdell, R. G.; Walsh, A.; McNulty, J.; Smith, K. E.; Piper, L. F. J. The Nature of Electron Lone Pairs in $BiVO_4$. *Appl. Phys. Lett.* **2011**, *98*, 212110.

(23) Cheng, J.; Sprik, M. Alignment of Electronic Energy Levels at Electrochemical Interfaces. *Phys. Chem. Chem. Phys.* **2012**, *14*, 11245−11267.

(24) Oshikiri, M.; Boero, M. *Water Molecule Adsorption Properties on the $BiVO_4$ (100) Surface* **2006**, *4*, 9188−9194.

(25) Oshikiri, M.; Boero, M.; Matsushita, A.; Ye, J. Water Molecule Adsorption Properties on Surfaces of MVO_4 (M = In, Y, Bi) Photo-Catalysts. *J. Electroceramics* **2007**, *22*, 114−119.

(26) Walsh, A.; Yan, Y.; Huda, M. N.; Al-Jassim, M. M.; Wei, S.-H. Band Edge Electronic Structure of $BiVO_4$: Elucidating the Role of the Bi s and V d Orbitals. *Chem. Mater.* **2009**, *21*, 547−551.

(27) Zhong, M.; Hisatomi, T.; Kuang, Y.; Zhao, J.; Liu, M.; Iwase, A.; Jia, Q.; Nishiyama, H.; Minegishi, T.; Nakabayashi, M.; et al. Surface Modification of the CoO_x Loaded $BiVO_4$ Photoanodes with Ultrathin p-Type NiO Layers for the Improved Solar Water Oxidation. *J. Am. Chem. Soc.* **2015**, *137*, 5053−5060.

(28) Ravensbergen, J.; Abdi, F. F.; van Santen, J. H.; Frese, R. N.; Dam, B.; van de Krol, R.; Kennis, J. T. M. Unraveling the Carrier Dynamics of $BiVO_4$: A Femtosecond to Microsecond Transient Absorption Study. *J. Phys. Chem. C* **2014**, *118*, 27793−27800.

(29) Otani, M.; Hamada, I.; Sugino, O.; Morikawa, Y.; Okamoto, Y.; Ikeshoji, T. Electrode Dynamics from First Principles. *J. Phys. Soc. Jpn.* **2008**, *77*, 024802.

(30) Schnur, S.; Groß, A. Challenges in the First-Principles Description of Reactions in Electrocatalysis. *Catal. Today* **2011**, *165*, 129−137.

(31) Eisenberg, D.; Ahn, H. S.; Bard, A. J. Enhanced Photo-electrochemical Water Oxidation on Bismuth Vanadate by Electro-deposition of Amorphous Titanium Dioxide. *J. Am. Chem. Soc.* **2014**, *136*, 14011−14014.